

Control system with a non-parametric predictive algorithm for a high-speed rotating machine with magnetic bearings

Paulina KURNYTA-MAZUREK^{1*}, Tomasz SZOLC², Maciej HENZEL¹, and Krzysztof FALKOWSKI¹

¹Faculty of Mechatronics, Armament and Aerospace, Military University of Technology,
ul. gen. Sylwestra Kaliskiego 2, 00-908, Warsaw, Poland

²Institute of Fundamental Technological Research, Polish Academy of Science, ul. Adolfa Pawińskiego 5B, 02-106, Warsaw, Poland

Abstract. This paper deals with research on the subject of magnetic bearing control systems for a high-speed rotating machine. Theoretical and experimental characteristics of the control systems with the model algorithmic control (MAC) algorithm and the proportional-derivative (PD) algorithm are presented. The MAC algorithm is the non-parametric predictive control method that uses an impulse response model. A laboratory model of the rotor-bearing unit under study consists of two active radial magnetic bearings and one active axial (thrust) magnetic bearing. The control system of the rotor position in air gaps consists of the fast prototyping control unit with a signal processor, the input and output modules, power amplifiers, contactless eddy current sensors and the host PC with dedicated software. Rotor displacement and control current signals were registered during investigations using a data acquisition (DAQ) system. In addition, measurements were performed for various rotor speeds, control algorithms and disturbance signals generated by the control system. Finally, the obtained time histories were presented, analyzed and discussed in this paper.

Key words: magnetic bearing; predictive algorithm; high speed rotating machine.

1. INTRODUCTION

In recent years, innovative bearing technologies were developed and implemented in many industrial applications. Novel solutions, such as gas bearings [1] and magnetic bearings solved many restrictions and disadvantages of classic rotor-bearing systems during operational practice. Immense efforts were undertaken to implement the magnetic support technology in high-speed rotating machinery. This technology has invaluable advantages in friction reduction in turbomachinery, compressors, generators, etc. [2–6]. Compared with classical mechanical bearings, the magnetic support technology provides benefits such as the low amplitude level of rotor lateral vibrations, high durability, no mechanical contact between operation elements, i.e. the rotor and the stator, and long-term high-speed running ability [7, 8]. These features give the magnetic bearings considerable potential to become a key element in rotating machines [9].

In classic rotating machines, some inefficiency occurring during their operation, e.g. damages of the bearing elements without additional (external) diagnostic systems, is often almost undetectable. Therefore, careful selection of the bearing system to support a high-speed rotor is carried out already at the design stage. This is usually based on the load capacity, durability and operating condition parameters. Unfortunately, bearings are still often damaged without previous symptoms arising during oper-

ation. Therefore, a significant problem lies in the developing of modern bearing designs with high diagnostic capacity. Such possibilities can be obtained by means of an active magnetic suspension system.

Applying the active magnetic bearing technology in high-speed rotating machinery can overcome the physical limitations of the classic bearings. This technology allows us for a decrease of stiffness and for an increase of the damping ability of the radial bearings, which in turn reduces critical rotor speed values. Active magnetic bearings allow for precise control of the rotor position and enable monitoring “online”, diagnosing and identifying the high-speed rotating machines operation [10]. An effective control system, with a proper controller, should be designed to ensure strictly defined control quality indicators.

In general, magnetic bearing control systems are mostly limited to applying proportional-integral-derivative (PID) controllers [11, 12]. In monograph [11], overviews of magnetic bearings and bearingless electric drives are presented. The principle of operation and mathematical models of active magnetic suspensions (AMS) and the controller design based on the PID algorithm are also described. Additionally, in that monograph, synchronous and asynchronous bearingless electric motors are presented in detail. Finally, monograph [12] discusses the magnetic bearing design procedure, the advantages of magnetic bearing systems in rotating machines, PID controller design methodology for the magnetic suspension control systems and their hardware implementation.

Furthermore, paper [13] presents a computer model of an active magnetic bearing used to determine a distribution of the

*e-mail: paulina.mazurek@wat.edu.pl

Manuscript submitted 2021-03-31, revised 2021-07-02, initially accepted for publication 2021-07-29, published in December 2021

magnetic field. As a result, values of the electromagnetic force and the magnetic flux density were applied for the AMS non-linearity analysis. On the other hand, in [14], an analysis of the magnetic field distribution of an active magnetic bearing was carried out employing the finite element method (FEM). The computational results obtained were then experimentally verified and analyzed. Additionally, paper [10] presents a procedure for experimental identification of dynamic parameters of an active magnetic bearing.

Other types of control systems were also investigated in the literature. Namely, studies of magnetic bearing control systems with robust controllers are presented in papers [15, 16]. In paper [15], the flywheel control system with an active magnetic bearing (AMB) and a robust controller were shown. Additionally, a design methodology of optimal controller H_{opt} was characterized, taking account of the uncertainties and nonlinearities of the model. The procedure for selecting weighting functions and reducing control laws was described in that paper as well. Paper [16] presents the control system of a homopolar magnetic bearing with permanent magnets and the control system based on H_2 , H_{inf} , H_{opt} robust algorithms. The obtained system's registered time responses and frequency characteristics were demonstrated in this study and compared with similar results obtained using the PID controller.

Additionally, in [17], a comparison between two control algorithms dedicated to the control system of radial active magnetic bearings was presented. In this monograph, the pole-placement control and sliding control methods were introduced and applied. That paper also presents a collation of experimental results. However, an application of robust control methods may lead to overestimations of parametric and non-parametric noise levels in the models, which are difficult to measure and cause incorrect control signals. For that reason, in that paper, the predictive control method was proposed. In this approach, a predictive control process with a strictly defined reference trajectory results in a distinctly smaller variation of the control signal and it also avoids the saturation phenomenon. Additionally, during predictive controller synthesis, the object model is identified basing on time histories. Then, there is no need to know the exact object parameters necessary during the design of robust controllers.

Numerous studies were also carried out with the use of predictive controllers in AMB control systems. However, in [18] the published findings, which take account of the predictive control method, include only results of theoretical tests obtained by means of the magnetic suspension system with one degree of freedom. Therefore, the effects of implementation of the predictive control system in a magnetically suspended high-speed rotor are presented in that paper.

The predictive control methods can be applied to objects with structures that are inherently unstable, non-linear and non-stationary. According to a reference model, these methods are intended to find out a sequence of future values for the control signal. The algorithm developed enables stable and undisturbed operation of even non-linear and unstable objects. Predictive control methods are based on structural identification of the control plant [19]. They are divided into two groups: algorithms with

parametric identification and algorithms with non-parametric identification. The first algorithm group includes the extended horizon adaptive control (EHAC) algorithm, the extended prediction self-adaptive control (EPSAC) algorithm and the generalized predictive control (GPC) algorithm. The second group contains the model algorithmic control (MAC) algorithm, the model predictive control (MPC) algorithm and the dynamic matrix control (DMC) algorithm. The MAC algorithm assumes simple adaptive control with an impulse response model. In contrast, the MPC algorithm uses differential control with an impulse response model. However, using the DMC method, an algorithm for predictive control with a step response model is obtained.

The contents of this paper are organized as follows. In the first section, a laboratory model of a magnetically suspended rotor is introduced. Next, theoretical studies of control systems with predictive and PD algorithms are presented. Then, optimal parameters of the PD controller are found using the pole placement method described in [18, 20], experimentally tuned on a test rig. The third section presents a laboratory stand with a control system dedicated to the rotor-bearing system. Afterwards, some experimental results are presented along with their analysis. Finally, concluding remarks based on the achieved results are formulated.

2. MATHEMATICAL MODEL OF THE LABORATORY ROTOR SHAFT

Taking into account the geometric shape of the laboratory rotor shaft under study and the frequency range of dynamic processes to which it will be subjected, with sufficient accuracy for research purposes, this rotor can be represented by a rigid body with 4-degrees of freedom. These degrees of freedom correspond to four generalized coordinates, namely: two translational displacements of the rigid body gravity center in two mutually perpendicular directions to the axis of rotation, and two rotational displacements about the axes mutually perpendicular to the axis of rotation. This rotor shaft is supported by means of two active magnetic bearings, as shown in Fig. 1. A rotor shaft motion is described in the ortho-Cartesian stationary coordinate

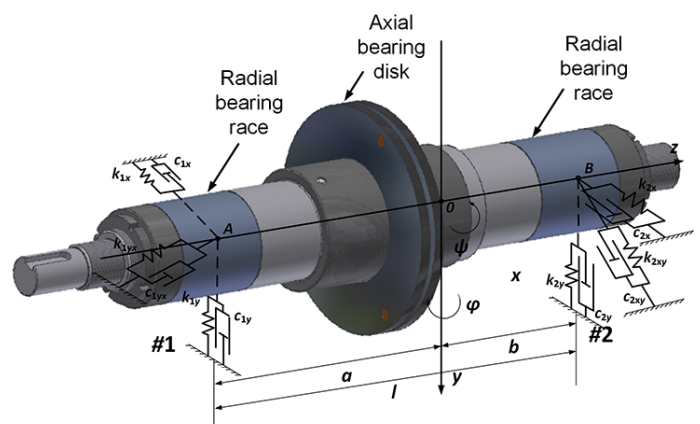


Fig. 1. Rigid-body model of the rotor shaft of high speed rotating machine suspended on active magnetic bearings

system $Oxyz$, the origin of which is attached to the rigid body gravity center. The Oz axis coincides with the bearing line, and the Oy and Ox axes are perpendicular to Oz in the vertical and horizontal direction, respectively. In Fig. 1, symbols a and b denote the distances from the gravity center O to the left-hand bearing #1 and the right-hand bearing #2, while factors k_{ix} , k_{iy} and c_{ix} , c_{iy} , $i = 1, 2$, are the stiffness and damping coefficients of both bearings' suspensions in the vertical and horizontal directions, respectively. Symbols k_{ixy} , k_{iyx} and c_{ixy} , c_{iyx} denote the cross-coupling components of the stiffness and damping coefficients. Viscoelastic parameters of the active magnetic bearings generally depend on the current stiffness coefficient, displacement stiffness coefficient and control law parameters [8]. In the case under study, when the PD control algorithm is applied, the coefficients of stiffness $k_{ix} = k_{iy}$ and damping $c_{ix} = c_{iy}$ of both magnetic bearings are equal to 2.88×10^5 N/m and 900.96 Ns/m, respectively, and the all cross-coupling coefficients k_{ixy} , k_{iyx} and c_{ixy} , c_{iyx} are equal to zero, $i = 1, 2$.

The equations of motion of this model derived using Lagrange's equations of the second kind, while bearing in mind the gyroscopic effects related to the shaft rotation, have the following form:

$$\mathbf{M} \cdot \ddot{\mathbf{r}}(t) + (\mathbf{C} + \Omega \mathbf{G}) \cdot \dot{\mathbf{r}}(t) + \mathbf{K} \cdot \mathbf{r}(t) = \mathbf{F}(t, \Omega^2), \quad (1)$$

where $\mathbf{r}(t) = \text{col} [y(t), x(t), \psi(t), \varphi(t)]$ denotes the vector of generalized coordinates corresponding, respectively, to translational displacements of the rotor-shaft gravity center along the axis Oy and Ox and to angular displacements around these axes, where Ω is the rotor constant angular velocity. Symbols \mathbf{M} , \mathbf{G} , \mathbf{C} and \mathbf{K} denote the matrices of inertia and gyroscopic effects and the matrices of damping and stiffness of the bearing suspension, respectively. All forcing terms are contained within the external excitation vector $\mathbf{F}(t, \Omega^2)$. Analogous equations of motion of the rigid rotor with four degrees of freedom, but without the cross-coupling terms in the damping and stiffness matrices, can be found e.g. in [21]. The presented mathematical model will be applied for numerical tests of rotor motions using the PD and predictive control algorithms being designed here.

3. PREDICTIVE CONTROL METHOD AND THEORETICAL RESULTS

Over the last few decades, the MPC predictive control method has become a prevalent research topic [22, 23], attracting attention among the control engineering community. This was caused by the fact that the computational power of a micro-processor continues to be strong and is still growing. Generally, the predictive control method uses a model of the object under consideration to predict future system states values [24, 25]. A prediction of the future values of the output signal $\check{y}(i+j)$, $j = 1, \dots, H-1$, is made for the prediction horizon H and the control signal value $u(i+j)$, $j = 1, \dots, L-1$, for the control horizon L at time i . This algorithm works to fulfil the control target, e.g. the control error minimum. For the correct operation of a predictive control algorithm, the assumption $L \geq H$ must be satisfied.

Predictive control algorithms belong to advanced control methods. They are characterized by low sensitivity to changes of object parameters and are used with oscillating, non-linear and non-stationary objects. The purpose of predictive control is to determine a sequence of future values of the control signal. According to the reference model, the control process is carried out through an appropriately defined reference trajectory for the output quantity, taking into account future changes of the reference value.

As mentioned above, predictive algorithms are based on several control methods. In this paper, a methodology of determining the MAC algorithm was presented as an example of non-parametric predictive controller synthesis [26]. This algorithm adopts the control system model in the following form:

$$y(i) = Vu(i-1), \quad (2)$$

where V is the polynomial whose coefficients are the impulse response values of the B/A element. The polynomial coefficients v_0, v_1, \dots, v_n are determined from (2) in the form of the product of the discrete object transfer function and the Z -transform of the discrete Dirac impulse. Assuming the discrete delay time equal to 1 and the object model with the autoregressive part, the polynomial V can be determined from the following relationship:

$$V = \frac{B}{A}. \quad (3)$$

The primary goal of the MAC algorithm is to minimize the divergence between the output signal prediction \check{y} and the reference w according to the following cost function:

$$J = \sum_{j=1}^H \{ [\check{y}(i+j) - w(i+j)]^2 + \rho u^2(i+j-1) \}. \quad (4)$$

To design the MAC control algorithm, firstly, the coefficients of polynomial V described by equation (3) should be determined, and then matrices Q and q ought to be composed:

$$Q = \begin{bmatrix} v_0 & 0 & \dots & 0 \\ v_1 & v_0 & \dots & 0 \\ \vdots & \vdots & \ddots & \vdots \\ v_{L-1} & v_{L-2} & \dots & v_0 \\ \vdots & \vdots & \ddots & \vdots \\ v_{H-1} & v_{H-2} & \dots & v_{H-L} \end{bmatrix}, \quad (5)$$

$$\mathbf{q}^T = [q_1, q_2, \dots, q_H] = \bar{\mathbf{i}}^T [\mathbf{Q}^T \mathbf{Q} + \rho \mathbf{I}]^{-1} \mathbf{Q}^T. \quad (6)$$

The polynomials R , S and T of the controllers take the following form:

$$R = 1 + z^{-1} \sum_{j=1}^H q_j (V_j^2 - V), \quad (7)$$

$$T = K_m \sum_{j=1}^H q_j, \quad (8)$$

$$S = \sum_{j=1}^H q_j, \quad (9)$$

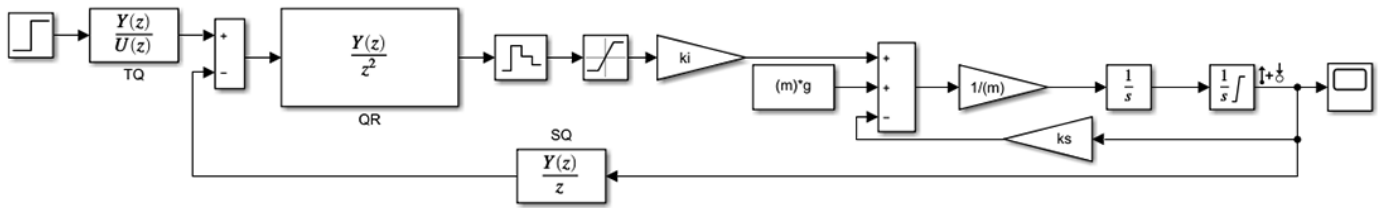


Fig. 2. Scheme of the control system applied to the model with one degree of freedom

while the control algorithm is described by the following equation:

$$Ru(i) = Tw(i) - Sy(i) \tag{10}$$

In turn, coefficient K_m to be found in equation (8) defines the reference trajectory. It is determined by the ratio of polynomials B_m and A_m . Usually, the first order trajectory can be calculated from the following relation:

$$K_m = \frac{B_m}{A_m} = \frac{(1 - \rho)z^{-1}}{1 - \rho z^{-1}}, \tag{11}$$

where ρ is the controller tuning parameter that determines its speed, i.e. $0 < \rho < 1$.

Based on equations (2)–(11), MAC controller polynomials R , S and T were calculated for the rotor-bearing system shown in Fig. 1. The theoretically analyzed algorithms of the designed control system were implemented in MATLAB and Simulink software. Firstly, the single-degree-of-freedom system was analyzed, by means of which rotor motion was investigated in the vertical direction only. A scheme of the corresponding control system is presented in Fig. 2.

Responses in time of the rotor displacement and the control currents were obtained using the system presented in Fig. 2. The response of the rotor observed along the vertical Oy axis shown in Fig. 1 was also determined. The rotor has been loaded by the gravity force and the unit step signal. This signal was a reference trajectory and appeared after 100 ms in the form of kinematic excitation with the value of $2.5 \cdot 10^{-6}$ m. Time histories obtained using the analyzed control system are presented in Fig. 3 and Fig. 4.

In Fig. 3, the time histories of the vertical rotor displacement obtained using the control systems with the MAC algorithm and the control system with the PD controller are presented. The control system with the predictive algorithm is characterized by almost ten times smaller control error than the control system equipped with the PD algorithm. The proposed approaches have similarly transient processes, and the settling time of the predictive algorithm is shorter than in the control system with the PD algorithm.

Additionally, Fig. 4 shows time histories of the electric currents responsible for control of the vertical motion determined using the control system with the MAC algorithm and the control system with the PD controller. More severe oscillations of the current have been registered in the case of the control system with the predictive algorithm than in the case of the standard system with the PD controller. As a result, the predictive

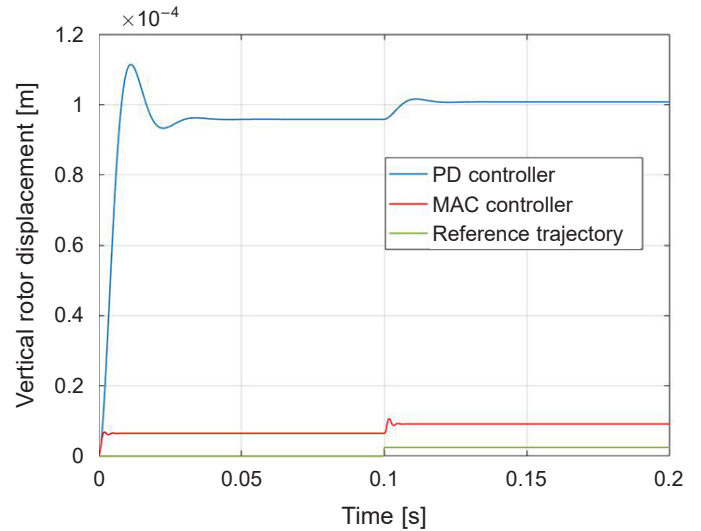


Fig. 3. Time histories of the vertical rotor displacement obtained using the tested control systems

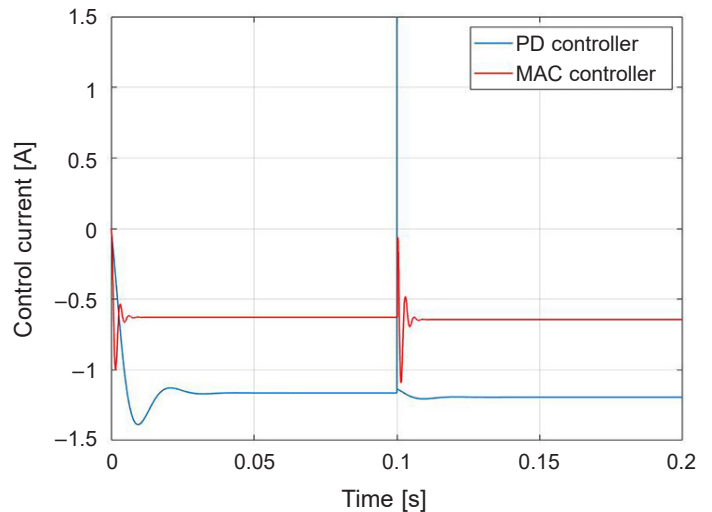


Fig. 4. Time histories of the electric current responsible for to control the vertical motion determined using the control systems with the MAC and the PD controllers

system is saturated for a longer time, but this difference is only slight. Additionally, a steady level of control current is lower than in the case of the PD controller. In summary, it turned out that the predictive control system worked better than the standard one. In the next part of this paper experimental studies of the non-parametric algorithm will be performed.

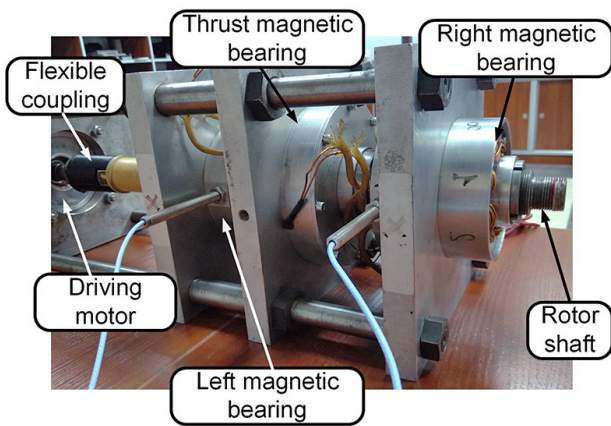


Fig. 5. The magnetic suspension system of the laboratory rotor-shaft

4. LABORATORY TEST-RIG AND EXPERIMENTAL RESULTS

The magnetic suspension system of the laboratory rotor-shaft was used for studies of predictive control algorithms. This system is presented in Fig. 5, and it consists of two active radial magnetic bearings and one axial (thrust) bearing. Each of the active radial magnetic bearings can generate a maximum electromagnetic force of 400 N. Air gaps in the radial and axial magnetic bearings are equal to 0.25 mm and 0.3 mm. Thus, the operating point current for each bearing is equal to 4 A at the maximum current value of 8 A. The radial magnetic bearings have 30 windings, whereas the axial one has 60 windings. Eddy current sensors are located in the electromagnet covers. Signals from these sensors provide information about the rotor position for the closed-loop control system, which provides fundamental data for the correct operation of a diagnostic system. The principal parameters of the bearing system and the control algorithm are presented in the Appendix.

A scheme of the magnetic bearing suspension control system in the laboratory rotor-shaft is presented in Fig. 6. It consists of the control unit, amplifiers, electromechanical actuators of the

supported rotor-shaft and the eddy current sensors. The control unit is based on a PC and dSpace platform with input/output cards with 16-bits A/D and D/A converters. The control algorithms were designed in MATLAB and Simulink software and then they were implemented in the dSPACE platform employing Matlab Real-Time Workshop (RTW) toolbox.

Within experimental studies, step responses were analyzed using the predictive control system with the MAC algorithm. Initially, responses in time due to a unit step signal were obtained at zero rotational speed of the rotor. This signal created a reference trajectory in the form of a square wave with an amplitude of $2.5 \cdot 10^{-6}$ m and frequency of 1 Hz. Time responses due to an impact of the input (reference) signal acting in the air gap in the vertical direction have been registered at the left- and right-hand bearings, where the MAC predictive algorithm was applied. These results are presented in Fig. 7. Here, the refer-

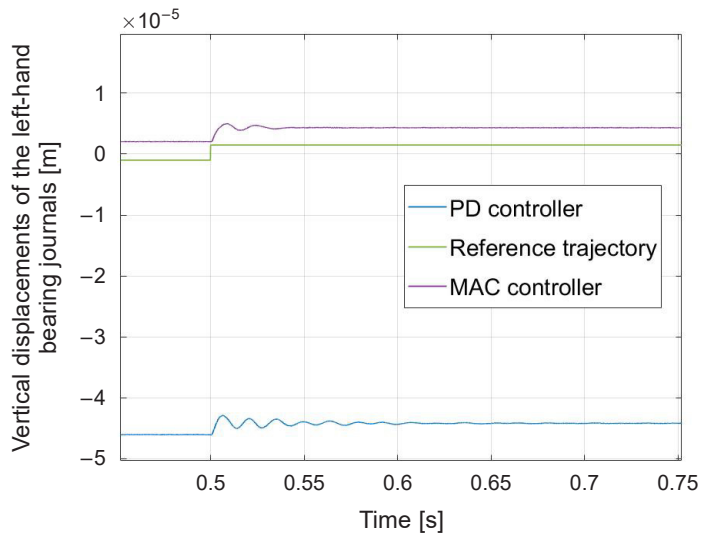


Fig. 7. Vertical displacements of the left-hand bearing journals obtained using the control algorithms being tested

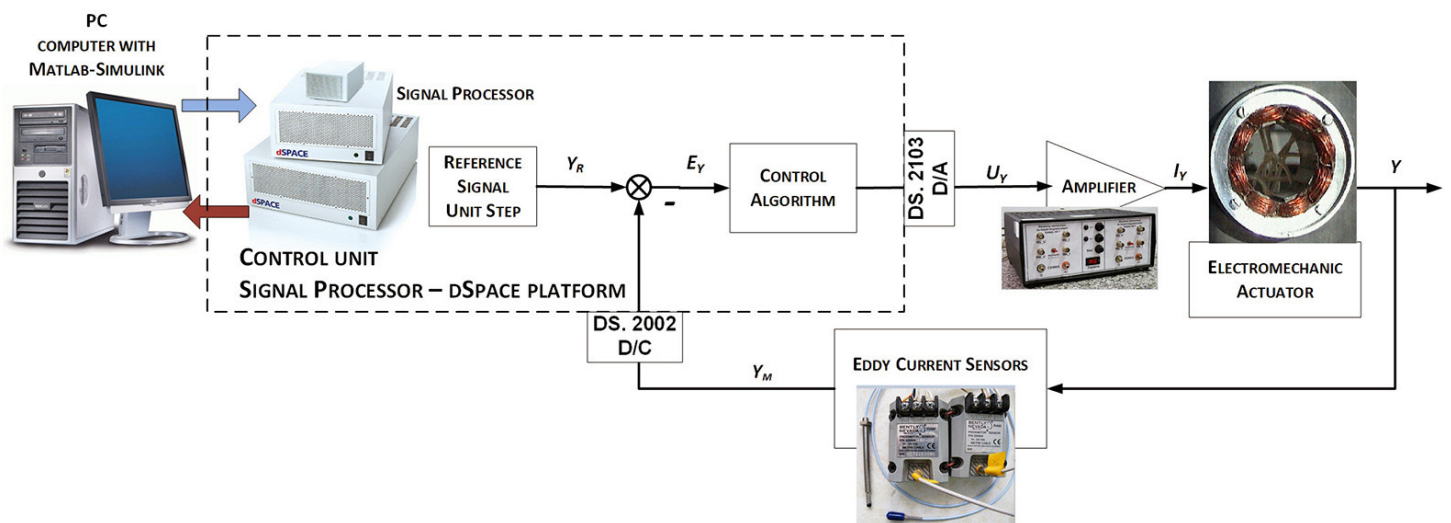


Fig. 6. Scheme of the control system of the magnetic bearing suspension of the laboratory rotor-shaft, [5, 9]

ence signal is marked using the green line. In this time history diagram the analogous response obtained by means of the PD controller is marked using the blue line to compare control quality of the standard and the predictive control system. A time history of vertical displacement of the left-hand bearing journal is presented in Fig. 7. The MAC algorithm is characterized by a settling time of approximately 25 ms. In turn, the value of maximum overshoot A is equal to 27%. In the case of the control system with the PD controller, the settling time and overshoot A have values of 100 ms and 70%. The time history of the vertical displacement of the right-hand rotor-shaft bearing journal is presented in Fig. 8. The predictive control systems with the MAC algorithm are characterized by the settling time equal to 50 ms. The value of maximum overshoot A is equal to 29%. Here, the use of the control system with the PD controller resulted in the control time and overshoot A of about 250 ms and 95%, respectively.

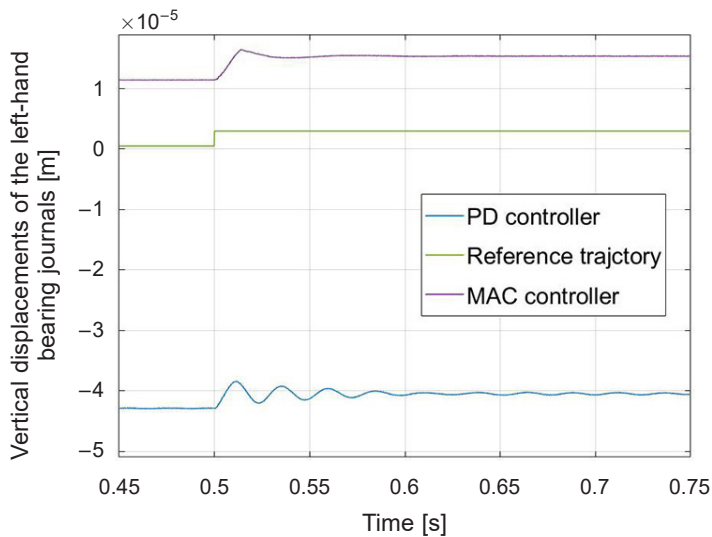


Fig. 8. Vertical displacements of the right-hand bearing journal obtained using the control algorithms being tested

Time histories of the control current responsible for stabilizing vertical motion of the left- and right-hand rotor-shaft bearing journal are appropriately presented in Fig. 9 and in Fig. 10, respectively. Measurements of this control current were made using the standard control systems with the PD controller and the control system with the predictive algorithm. Here, operation of the standard control system is characterized by the highest value of current changes. The smallest amplitudes of current changes characterizes operation of the control system with the MAC controller.

In the case of time history of the control current in the right-hand bearing presented in Fig. 10, operation of the control system with the PD controller is also characterized by the largest value of current changes. Applying the control system with the MAC controller leads similarly to the largest value of the current value and the smallest amplitudes of current changes.

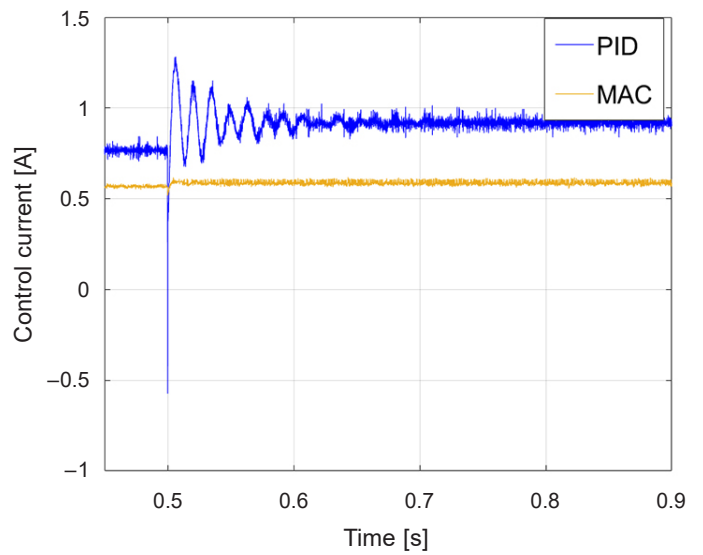


Fig. 9. Time histories of the left-hand bearing current responsible for controlling vertical motion obtained using the control algorithms being tested

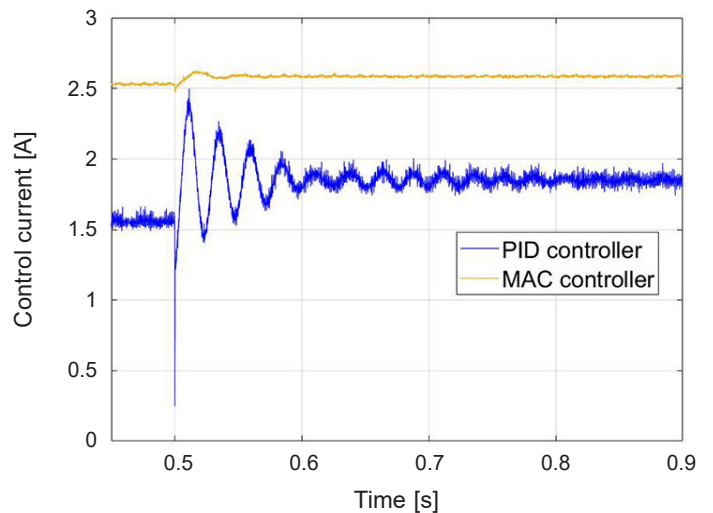


Fig. 10. Time histories of the right-hand bearing current responsible for controlling vertical motion obtained using the control algorithms being tested

In the following stages of experimental research, time histories of the left-hand rotor-shaft bearing journal displacements in the vertical direction at constant rotational speeds were recorded. Consequently, in Fig. 11 and Fig. 12 present registered time histories, FFT amplitudes and power spectrum characteristics of the rotor-shaft journal vertical displacement registered at the rotational speeds of 300 rpm and 2000 rpm, respectively.

Maximum amplitude values of rotor vibrations were noted for each of these time histories. Here, the smallest displacement of the left-hand bearing journal has been observed at 300 rpm, when the system with the PD controller was used. In turn, in the control system with the predictive algorithm, an amplitude of

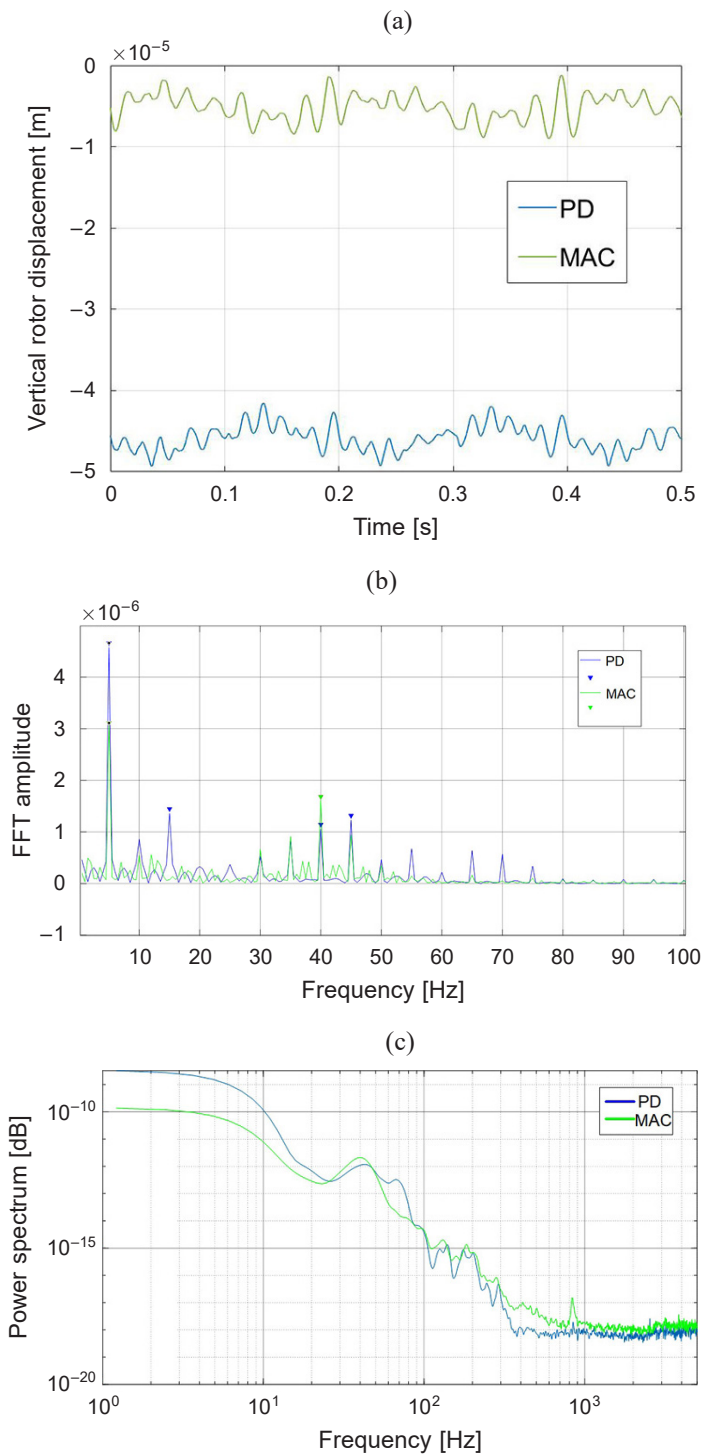


Fig. 11. Vertical displacements of the left-hand bearing journal obtained at the rotational speed of 300 rpm, a) time histories, b) FFT amplitude, c) power spectrum

ca. 10% larger value has been registered. However, the smallest vibration amplitude of the right-hand bearing journal vertical displacement was observed at 2000 rpm due to the predictive control algorithm MAC application, and the largest one has been registered when the control system with the PD algorithm was used.

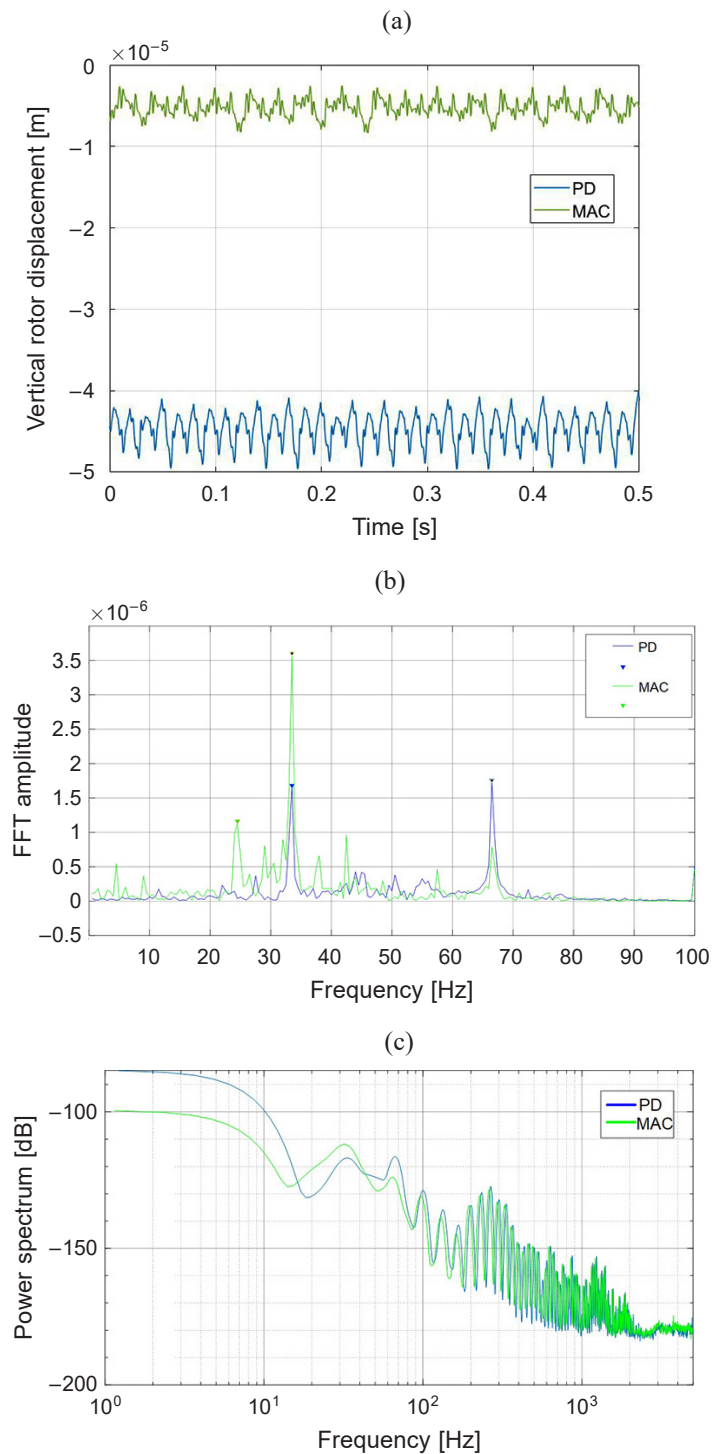


Fig. 12. Vertical displacements of the left-hand bearing journal obtained at the rotational speed of 2000 rpm, a) timehistories, b) FFT amplitude, c) power spectrum

5. CONCLUSIONS

The paper presents results of theoretical and experimental studies of predictive control systems dedicated to the high speed rotating machine with a rotor suspended by means of active magnetic bearings. For this purpose, a laboratory test-rig equipped with proper control systems has been built. Further-

more, measurements were performed for excitations in the form of a unit step signal at rotor-shaft zero rotational speed, and without excitation at constant rotational speeds, when various **advanced** control algorithms were used. The results of experimental research confirm qualitatively the findings obtained using the theoretical studies. Namely, in both cases, the control system with the PD controller resulted in a greater control error than the predictive control system. Moreover, peak values of the control currents were also more significant than those obtained using the MAC algorithm.

In the first stage of the predictive control system application, time histories of vertical displacements of the rotor bearing journals caused by the unit step signal were registered. Preliminary experiments have been obtained at zero rotational speed under excitation in the square waveform with an amplitude of $2.5 \cdot 10^{-6}$ m and frequency of 1 Hz. The parameters determining quality of the PD algorithm and advanced control algorithms are presented in Table 1.

Table 1
List of parameters determining control quality

	Parameter	PD	MAC
Left bearing	Settling time [ms]	100	25
	Overshoot [%]	70	27
	Control error in steady-state [m]	$4.6 \cdot 10^{-5}$	$7.5 \cdot 10^{-6}$
Right bearing	Settling time [ms]	250	50
	Overshoot [%]	95	29
	Control error in steady state [m]	$4.1 \cdot 10^{-5}$	$1.6 \cdot 10^{-5}$

Table 1 compares values of the settling time, overshoot and control error under steady-state operational conditions obtained using the different control algorithms, i.e. PD and MAC controllers. Here, in each experimental test, the standard system resulted in worse dynamic properties than the prediction one. The most significant difference was observed for the steady control error value, which was greater by one magnitude order in the case of the standard system with the PD controller than when the predictive control system was used. On the other hand, the predictive control system with the MAC algorithm resulted in the smallest overshoot and the shortest settling time.

Next, time histories of the vertical displacement of the left-hand bearing journal at constant rotational speeds were recorded. These tests were carried out at rotational speeds of 300, 600, 900, 1500 and 2000 rpm. For each of the registered responses, maximum values of the vibration peaks were registered and included in Table 2.

Table 2
Maximum values of vibration amplitudes at constant rotational speeds of the rotor

	Rotational speed [rpm]	PD	MAC
Left bearing	300	$7.984e-06$	$8.651e-06$
	600	$9.837e-06$	$7.310e-06$
	900	$6.062e-06$	$5.426e-06$
	1500	$6.085e-06$	$6.143e-06$
	2000	$1.052e-05$	$6.434e-06$

From this comparison, it follows that the predictive algorithm manifested better properties than the PD algorithm. At small rotational speeds, i.e. up to 300 rpm, the time histories of bearing journal displacements obtained using the standard algorithm were characterized by at least similar or smaller maximum amplitudes than those when the predictive system was applied. But with an increase of the rotational speed of the rotor, the analogous time histories of journal displacements registered when using the prediction system were characterized by smaller vibration amplitudes.

It must be remembered that magnetic suspensions are structurally unstable systems. Therefore, they need a control system, which assures stable suspension operation around an operational point. Determining controller settings is a complex process for the unstable system. Thus, within the framework of performed research different controllers were tested, and optimum controllers for the active magnetic suspensions were searched for. In this study, the predictive controller was compared to the PD controller. The PD algorithm is a standard type of controller in the automatic system applied for active magnetic bearings. Therefore, the comparison of predictive controllers with the PD controller is justified.

The presented results of tests analyses of predictive control systems confirm the legitimacy of their use and development in the magnetic suspension systems of high-speed rotating machines. The constructed laboratory test-rig for the magnetically suspended rotor-shaft, together with the positive effects of preliminary studies, have opened new perspectives for development of research devoted to magnetic bearing suspension systems of high-speed rotating machines. The results obtained during these studies are the basis for identifying and monitoring systems of rotors supported by active magnetic bearings. In further research in this field, dynamic behaviors at greater rotor speeds will be investigated when using other types of advanced algorithms, e.g. robust and slide controllers.

ACKNOWLEDGEMENTS

This research was co-funded by the National Centre for Research and Development as the grant titled “The use of surface engineering new technologies and magnetic bearings in the construction of a miniature turbine jet engine”.

This work was co-financed by the Military University of Technology under research project UGB 899.

APPENDIX

Table 3

Numerical parameters of the laboratory rotor-shaft

Parameter	Symbol	Value	Unit
Mass of rotor	m	5.6	kg
Polar moment of inertia	I	0.0246	kg · m ²
Diametral moment of inertia	I_0	$2.736 \cdot 10^{-3}$	kg · m ²
Bearing stiffness coefficient	k	$2.88 \cdot 10^5$	[N/m]
Bearing damping coefficient	c	900.96	[Ns/m]
Prediction horizon	H	10	[s]
AMB air gap	x_0	0.25	[mm]
Current work point	i_0	1.5	[A]
Rotor total length	l	0.373	[m]
Bearing span	$a + b$	0.238	[m]

REFERENCES

- [1] P.-H. Kuo, R.-M. Lee, and C.-C. Wang, "A High-Precision Random Forest-Based Maximum Lyapunov Exponent Prediction Model for Spherical Porous Gas Bearing Systems," *IEEE Access*, vol. 8, pp. 168079–168086, 2020, doi: [10.1109/ACCESS.2020.3022854](https://doi.org/10.1109/ACCESS.2020.3022854).
- [2] E. Brusa, "Semi-active and active magnetic stabilisation of supercritical rotor dynamics by contra-rotating damping," *Mechatronics*, vol. 24, pp. 500–510, 2014, doi: [10.1016/j.mechatronics.2014.06.001](https://doi.org/10.1016/j.mechatronics.2014.06.001).
- [3] O. Halminen, A. Kärkkäinen, J. Sopanen, and A. Mikkola, "Active magnetic bearing-supported rotor with misaligned cageless backup bearings: A dropdown event simulation model," *Mech. Syst. Signal Process.*, vol. 50–51, pp. 692–705, 2015, doi: [10.1016/j.ymssp.2014.06.001](https://doi.org/10.1016/j.ymssp.2014.06.001).
- [4] J.Y. Hung, G.A. Nathaniel, and F. Xia, "Non-linear control of a magnetic bearing system," *Mechatronics*, vol. 13, pp. 621–637, 2003, doi: [10.1016/S0957-4158\(02\)00034-X](https://doi.org/10.1016/S0957-4158(02)00034-X).
- [5] J. Sawicki, E.H. Maslen, and K.R. Bischof, "Modeling and performance evaluation of machining spindle with active magnetic bearings," *J. Mech. Sci. Technol.*, vol. 21, pp. 847–850, 2007, doi: [10.1007/BF03027055](https://doi.org/10.1007/BF03027055).
- [6] R. Siva Srinivas, R. Tiwari, and Ch. Kannababu, "Application of active magnetic bearings in flexible rotordynamic systems – A state-of-the-art review," *Mech. Syst. Signal Process.*, vol. 106, pp. 537–572, 2018.
- [7] K. Falkowski, M. Henzel, and M. Żokowski, "The analysis of the control system for the bearingless induction electric motor," *J. Vibroeng.*, vol. 14, no. 1, pp. 16–21, 2012.
- [8] R. Stocki, T. Szolc, P. Tauzowski, and J. Knabel, "Robust design optimisation of the vibrating rotor shaft system subjected to selected dynamic constraints," *Mech. Syst. Signal Process.*, vol. 29, pp. 34–44, 2012, doi: [10.1016/j.ymssp.2011.07.023](https://doi.org/10.1016/j.ymssp.2011.07.023).
- [9] T. Szolc, K. Falkowski, M. Henzel, and P. Kurnyta-Mazurek, "Determination of parameters for a design of the stable electro-dynamic passive magnetic support of a high-speed flexible rotor," *Bull. Pol. Acad. Sci. Tech. Sci.*, vol. 67, no. 1, pp. 91–105, 2019, doi: [10.24425/bpas.2018.125719](https://doi.org/10.24425/bpas.2018.125719).
- [10] S. Zhe *et al.*, "Identification of active magnetic bearing system with a flexible rotor," *Mech. Syst. Signal Process.*, vol. 49, pp. 302–316, 2014.
- [11] A. Chiba *et al.*, *Magnetic bearings and bearingless drives*, Elsevier's Science Technology Rights Department in Oxford, UK, 2005.
- [12] G. Schweitzer, A. Traxler, and H. Bleuler, *Magnetlager: Grundlagen, Eigenschaften und Anwendungen berührungsfreier elektromagnetischer Lager*, Springer Verlag, Berlin, 1992.
- [13] A. Piłat, "Modelling, investigation, simulation, and PID current control of active magnetic levitation FEM model," *Methods and Models in Automation and Robotics (MMAR), 18th International Conference on Methods and Models in Automation and Robotics*, Poland, 2013, pp. 299–304, doi: [10.1109/MMAR.2013.6669923](https://doi.org/10.1109/MMAR.2013.6669923).
- [14] B. Tomczuk, J. Zimon, and K. Zakrzewski, "Integral parameters determination in the magnetic bearing using finite element method," *Computational Electromagnetics (CEM), 6th International Conference on Computational Electromagnetics*, Germany, 2006, pp. 1–4.
- [15] Z. Gosiewski and A. Mystkowski, "Robust control of active magnetic suspension: analytical and experimental results," *Mech. Syst. Signal Process.*, vol. 22, no. 6, pp. 1297–1303, 2008, doi: [10.1016/j.ymssp.2007.08.005](https://doi.org/10.1016/j.ymssp.2007.08.005).
- [16] M. Henzel and P. Mazurek, "The analysis of the control system of the active magnetic bearing," *Electrodynamic and Mechatronic Systems, 3rd International Students Conference on Electrodynamics and Mechatronics (SCE III)*, Opole, Poland, 2011, pp. 53–58, doi: [10.1109/SCE.2011.6092124](https://doi.org/10.1109/SCE.2011.6092124).
- [17] A.M. Beizama, J.M. Echeverria, M. Martinez-Iturralde, I. Egana, and L. Fontan, "Comparison between pole-placement control and sliding mode control for 3-pole radial magnetic bearings," *2008 International Symposium on Power Electronics, Electrical Drives, Automation and Motion*, 2008, pp. 1315–1320, doi: [10.1109/SPEEDHAM.2008.4581115](https://doi.org/10.1109/SPEEDHAM.2008.4581115).
- [18] Ch.Wu and Ch. Zhu, "Implicit generalised predictive control of an active magnetic bearing system," *17th International Conference on Electrical Machines and Systems*, Hangzhou, China, 2014, pp. 2319–2323.
- [19] K.S. Holkar and L.M. Waghmare, "An overview of model predictive controller," *Int. J. Control Autom.*, vol. 3, no. 4, pp. 47–64, 2010.
- [20] A.D. Lewis, *A Mathematical Approach to Classical Control*, Queen's University, Canada, 2003.
- [21] G. Genta, *Dynamics of Rotating Systems*, Springer Science + Business Media, Inc., Mechanical Engineering Series, 2005.
- [22] A. Ammar *et al.*, "An experimental assessment of direct torque control and model predictive control methods for induction machine drive," *International Conference on Electrical Sciences and Technologies in Maghreb*, Algiers, 2018, pp. 1–6, doi: [10.1109/CISTEM.2018.8613419](https://doi.org/10.1109/CISTEM.2018.8613419).
- [23] K.T. Wrobel, K. Szabat, and P. Serkies, "Long-horizon model predictive control of induction motor drive," *Arch. Electr. Eng.*, vol. 68, no. 3, pp. 579–593, 2019.
- [24] P. Kurnyta-Mazurek, A. Kurnyta, and M. Henzel, "Analysis of the method of predictive control applicable to active magnetic suspension systems of aircraft engines," *Research Works of Air Force Institute of Technology*, vol. 37, pp. 195–206, 2015, doi: [10.1515/afit-2015-0034](https://doi.org/10.1515/afit-2015-0034).
- [25] A. Niederliński, J. Mościński, and Z. Ogonowski, *Adaptive control*, Scientific Publisher PWN, Warsaw, 1995 [in Polish].
- [26] P. Kurnyta-Mazurek, T. Szolc, M. Henzel, and K. Falkowski, "Analysis of control methods for the jet engine rotor with magnetic bearings," *Proceedings of 14th International Conference on SIRM 2021 – Dynamics of Rotating Machines*, Gdansk, Poland, 2021.